Rho-Kinase Inhibition Ameliorates Non-Alcoholic Fatty Liver Disease in Type 2 Diabetic Rats

Hany A. ELKATTAWY[1,2], Dalia MAHMOUD ABDELMONEM ELSHERBINI[3,4], Hasnaa ALI EBRAHIM[5], Doaa M. ABDULLAH[6], Sheren A. AL-ZAHABY[7], Yousef NOSERY[8], Ahmed EL-SAYED HASSAN[2,9]

[1]Department of Basic Medical Sciences, College of Medicine, Almaarefa University, Riyadh, Kingdom of Saudi Arabia, [2]Medical Physiology Department, College of Medicine, Zagazig University, Egypt, [3]Department of Clinical Laboratory Sciences, College of Applied Medical Sciences, Jouf University, Sakaka, Kingdom of Saudi Arabia, [4]Department of Anatomy, Faculty of Medicine, Mansoura University, Mansoura, Egypt, [5]Department of Basic Medical Sciences, College of Medicine, Princess Nourah bint Abdulrahman University, Riyadh, Kingdom of Saudi Arabia, [6]Clinical Pharmacology Department, College of Medicine, Zagazig University, Egypt, [7]Zoology Department, College of Sciences, Zagazig University, Egypt, [8]Pathology Department, College of Medicine, Zagazig University, Egypt, [9]Department of Basic Medical Sciences, College of Medicine, Sulaiman AlRajhi University, Kingdom of Saudi Arabia

Summary

Non-alcoholic fatty liver disease (NAFLD) is linked to type 2 diabetes mellitus (T2DM), obesity, and insulin resistance. The Rho/ROCK pathway had been involved in the pathophysiology of diabetic complications. This study was designed to assess the possible protective impacts of the Rho/Rho-associated coiled-coil containing protein kinase (Rho/ROCK) inhibitor fasudil against NAFLD in T2DM rats trying to elucidate the underlying mechanisms. Animals were assigned into control rats, non-treated diabetic rats with NAFLD, and diabetic rats with NAFLD that received fasudil treatment (10 mg/kg per day) for 6 weeks. The anthropometric measures and biochemical analyses were performed to assess metabolic and liver function changes. The inflammatory and oxidative stress markers and the histopathology of rat liver tissues were also investigated. Groups with T2DM showed increased body weight, serum glucose, and insulin resistance. They exhibited disturbed lipid profile, enhancement of inflammatory cytokines, and deterioration of liver function. Fasudil administration reduced body weight, insulin resistance, and raised liver enzymes. It improved the disturbed lipid profile and attenuated liver inflammation. Moreover, it slowed down the progression of high fat diet (HFD)-induced liver injury and reduced the caspase-3 expression. The present study demonstrated beneficial amelioration effect of fasudil on NAFLD in T2DM. The mechanisms underlying these impacts are improving dyslipidemia, attenuating oxidative stress, downregulated inflammation, improving mitochondrial architecture, and inhibiting apoptosis.

Corresponding author

H. A. Elkattawy, Department of Basic Medical Sciences, College of Medicine, Almaarefa University, P.O. Box 71666, Riyadh, Kingdom of Saudi Arabia. E-mail: hmohammed@mcst.edu.sa

Introduction

Diabetes mellitus induces derangement in metabolism of carbohydrate, lipid, and protein, resulting in major problems such as blindness, renal failure, hepatic damage, nerve injury, and atherosclerosis [1].

NAFLD is a set of hepatic abnormalities that range from basic hepatic steatosis to fulminant symptoms including inflammation and hepatic damage, known as nonalcoholic steatohepatitis (NASH), which can result in cirrhosis, hepatic carcinoma, and eventually hepatic failure [2-4]. Many patients with T2DM develop NAFLD with its inflammatory complication, NASH [5]. Insulin resistance, lipid peroxidation, mitochondrial dysfunction, and oxidative stress are all implicated in the pathophysiology of NAFLD [6,7].

Rho-kinase has been considered one of the responsive proteins of the guanosine triphosphate (GTP)-binding protein; RhoA. RhoA/Rho-kinase pathway has a major role in many cellular physiological functions, like contraction of smooth muscles, motility, and cell adhesion [8]. Hepatic ROCK1 is significantly increased in individuals with hepatosteatosis and is associated with some risk factors that cluster around resistance to insulin and NAFLD. It was also stated that liver ROCK1 inhibit AMP-activated kinase (AMPK) activity; a crucial molecule of metabolism [9]. Additionally, AMPK enhances the uptake of glucose, oxidation of lipid, and mitochondrial bio-formation in skeletal muscles, while in liver, it suppresses glucose output and synthesis of lipid and enhances lipid oxidation [10]. Rho-kinases have been assembled to several diabetes-induced pathophysiological signals and were stated as hopeful molecular targets for reno-protective therapy [11]. While the influence of Rho-kinase signaling in diabetic hepatic injury has been scarcely explored. Therefore, in the current work, we explored the predictive liver protective impacts of fasudil, the Rho/ROCK inhibitor in T2DM rat model with NAFLD.

Methods

Animals and protocol

Twenty-four Wistar healthy adult rats, weighing 150-180 g were procured from the animal house at the faculty of Veterinary Medicine, Zagazig University, Egypt. Under hygienic conditions, animals were housed in steel wire cages (3-4/cage) at room temperature, on a natural light/dark cycle with access to water freely and adapted to the new environment for one week before the beginning of the experiments. Following acclimatization, animals were divided randomly to have a standardized diet (57 % carbohydrate, 25 % protein, and 18 % fat) as a control group (n=8) or a high-fat diet (n=16) with high

amounts of corn oil, containing >98 % ω-6 poly unsaturated fat acid (PUFA) (HFD, 50 % fat, 38 % carbohydrate containing mainly fructose, and 12 % protein) for 6 weeks to induce obesity (the diets were purchased from Faculty of Agriculture, Zagazig University). A single low dose of streptozotocin (STZ) (30 mg/kg BW) (Sigma Aldrich Co., USA) dissolved in citrate buffer (pH 3.5) was intraperitoneally injected to rats within 20 min of preparation (at the end of the fifth week) [12,13]. Glucose levels were checked using a portable glucometer (Accu-Chek Active, Roche Diagnostics Limited, Germany) after 1 week of STZ injection in blood samples withdrawn from the tail vein. Rats with plasma glucose levels of ≥11.10 mmol/l were included in the study for the subsequent 6 weeks. Diabetic rats were randomly allocated to HFD+T2DM rats, (n=8); and HFD+T2DM+Fasudil rats (n=8) that received hydrochloride fasudil (10 mg/kg per day, intraperitoneal injection) (Tianjin Hongri Company, Tianjin, China) every day for another 6 weeks. The dose of fasudil was applied in accordance with previous study [12]. The control and HFD+T2DM groups received intraperitoneal injections of a sterile vehicle every day until the end of the experiment.

Measurement of anthropometric parameters

Body weight was measured in accordance with Nascimento *et al.* [14]. Rat length, abdominal circumference (AC) (the largest zone of the rat abdomen), and thoracic circumference (TC) (directly posterior to the foreleg) were assessed as described by Novelli *et al.* [15]. Body mass index (BMI): body weight (g)/length^2 (cm^2) and AC/TC ratio (representing an index of abdominal obesity) were calculated [15,16].

Blood biochemical analyses and liver lipid's extract for triglyceride (TG)

After an overnight fasting, serum was collected from retro-orbital blood samples after centrifugation at 1500×g for 20 min, and kept at -20 °C [17] to be processed for biochemical analysis. Serum glucose level (mmol/l) was determined colorimetrically using glucose colorimetric detection kit (Biosource Europe S.A. Belgium, Cat. No. EIAGLUC) as described by Ebrahim *et al.* [18], and serum insulin level (pmol/l) was assessed by rat insulin Enzyme-linked Immunosorbent Assay (ELISA) Kits (Sigma-Aldrich, Cairo, Egypt, Cat. No. EZRMI) as described by Sabir *et al.* [19]. The

standard curve range for insulin was 1.5-48 mIU/l with sensitivity of 0.1 mIU/l. By adding acidic solution, the reaction was terminated, and absorbance readings were noted at 450 nm on a multimode microplate reader (Synergy, USA). HOMA-IR (homeostasis model assessment-insulin resistance) index was applied to assess (HOMA-IR) according to the equation used by Bonora *et al.* [20]: HOMA-IR = fasting serum glucose (mg/dl) × fasting serum insulin (μIU/ml)/405. Serum total cholesterol (TC) and triglycerides (TG) levels were assessed by an enzymatic colorimetric method using specific cholesterol and triglycerides kits (Spinreact Spain, Cat. No. CHOD-POD and Cat. No. GPO-POD. respectively) and analyzed by a spectrophotometer with the absorbance was measured at 510 nm with a sample/reagent volume ratio as low as 1:150 as described by Fossati and Prencipe [21]. High-density lipoprotein-cholesterol (HDL-c) level was assessed by an enzymatic colorimetric method using HDL cholesterol assay kit (Biodiagnostic®, Cairo, Egypt, Cat. No. CH 12 30) with the absorbance was measured at 500 nm as described by Nauck *et al.* [22]. Serum low-density lipoprotein-cholesterol (LDL-c) level was assessed by using the Friedewald formula [23] as follows: LDL-c = TC - HDL - TG/5. Hepatic triglyceride (TG) level was assessed in accordance with Foster and Dunn [24] after tissue lipids extraction according to the method of Folch *et al.* [25]. A hepatic mixture of 25 mg frozen liver tissue, and 100 μl phosphate buffer saline (PBS) (w/v, pH 7.4), was added to 500 μl of an extracting solvent (chloroform and methanol; 2:1 ratio) for homogenization followed by centrifugation at 2500 rpm for 5 min at 4 °C. The supernatant was collected followed by washing of the mixture with 100 μl of 0.9 % normal saline (NS) at room temperature (RT), which was left for separation of its components into layers. The lipid lower layer was shifted to another test tube, and subjected to evaporation at 70 °C using a water bath. After drying, 10 μl of the mixture was added to 100 μl of PBS to measure TGs content using the conventional TGs kits (Sigma-Aldrich, Cairo, Egypt, Cat. No. MAK266) on biosystems bioanalyzer, the absorbance was measured at 570 nm and the unit was expressed as mg/g liver.

Alanine aminotransferase (ALT) and aspartate aminotransferase (AST) activity in the serum were assessed by sandwich enzyme-linked immunosorbent assay (ELISA) system. They were measured *via* a Rat ALT ELISA kit (Kamiya Biomedical Company, KT-6104, Gateway Drive, Seattle) and a Rat AST ELISA kit (Sunred Biological Technology, 201-11-0595, China), respectively, by the method of Vassault [26]. Serum albumin was assessed by using bromocresol green according to the method described by Wack and Warmolts [27]. Serum tumor necrosis factor α (TNF-α) concentration was assessed by TNF-α (Rat) ELISA kits purchased from ALPCO (45-TNFRT-E01.1). The standard curve range for TNF-α was 10-320 pg/ml with a 1.0 pg/ml sensitivity. By adding acidic solution, the reaction was terminated, and absorbance readings were noted at 450 nm on a multimode microplate reader (Synergy, USA). The high sensitivity C-reactive protein (hs-CRP) level was assessed using ELISA kit (Cat. No. ERC1021-1; ASSAYPRO, USA) according to manufacturer-provided standards and protocols [28].

Hepatic Oxidative Stress (OS) markers

Liver tissues were processed to obtain a 10 % homogenate (w/v) in a 20 mM cold aminomethane (hydroxymethyl) buffer (pH 7.4). Supernatants were collected after centrifugation of homogenates at 1,500× g for 30 min at 4 °C to estimate oxidative stress markers. Malondialdehyde (MDA) as a lipid peroxidation indicator was measured using bio diagnostic kit according to Varshey and Kale [29]. Hepatic superoxide dismutase (SOD) was assessed using phenazine methosulfate (PMS) depending on nitro-blue tetrazolium inhibition as described by Misra and Fridovich [30]. According to Rajurkar *et al.* [31], the activity of glutathione S-transferase (GST) was estimated with the help of 1-chloro-2,4-dinitrochlorobenzene. A GST unit is defined as 1 mol of CDNB-GSH conjugate formed/min/mg protein. Glutathione Peroxidase (GPx) activity assay of liver extract was assessed in accordance with the method applied by Paglia and Valentine [32] with partial modification. Simply, the method was based on peroxides reduction at 340 nm in the existence of nicotinamide adenine dinucleotide phosphate (NADPH). One unit (U) of GPx activity was defined as the quantity of enzyme needed to catalyze the oxidation of 1 nM NADPH for one minute. Kits for MDA (Cat. No. MAK085), SOD (Cat. No. 19160), GST (Cat. No. MAK453), and GPx (Cat. No. MAK437) were bought from Spectrum Co. (Sigma-Aldrich, Cairo, Egypt).

Histopathological evaluation of liver tissue

Fresh livers were excised and weighed to

estimate liver index (% = liver weight/body weight × 100) then processed for histopathological examinations. 10 % buffered formalin was used to fix liver specimens for 48-60 h followed by processing in ethyl alcohol and xylene series to prepare paraffin blocks. Hematoxylin and eosin (H&E) stained sections (5 µm thick) of hepatic tissue were prepared to examine the hepatic architectural changes [33]. The pathologist assessed and scored the stained specimens blindly using an optical microscope with attached camera. NAFLD histological scoring was based on the NAFLD Activity Score (NAS) nominated by The Pathological Committee of the NASH Clinical Research Network [34]. The scores were the summation of the following scores: Steatosis (0=<5 %, 1=5-33 %, 2=34-66 %, 3=>66 %), lobular inflammation (0=no foci, 1=<2 foci per 200× field, 2=2-4 foci per 200× field, 3=>4 foci per 200× field), and ballooning (0=none, 1=rare or few, 2=many or prominent). A NAS score ≥5 was defined as NASH; 2<NAS<5 was defined as borderline NASH, and NAS≤2 was simple steatosis [35]. Evaluation of Liver fibrosis was conducted using Sirius red stained liver sections. Slides were incubated overnight with 0.1 % Sirius red (Sigma-Aldrich, UK), treated with 0.01 M hydrochloric acid and followed by dehydration in serial ethanol concentrations without water. The Image J software was used to measure the area percentage of fibrosis in Sirius red-stained hepatic sections. The fibrosis score was also done using a five-point scale (0 no fibrosis, 1 fibrosis encircling portal area with no septa, 2 few septa, 3 multiple septa with no cirrhosis, 4 cirrhosis), which was discussed by previous research work [36].

Immunohistochemical staining with anti-caspase-3 antibody

Apoptotic areas were demonstrated in anti-caspase-3 antibody immunostained liver slides (Cat. No. ab4051, Abcam, USA). Phosphate-buffered saline was applied for deparaffinized section after incubation with 3 % hydrogen peroxide at room temperature for 10 min to mask the endogenous peroxidase activity. A primary antibody (biotinylated goat anti-rabbit antibody diluted 1:200 at room temperature for one hour) was incubated with liver sections overnight to detect the presence of apoptosis markers. Lastly, liver slides were counterstained with hematoxylin and dehydrated in ethanol then eventually mounted with DPX [37]. Microscopically, positive immunoreactivity for caspase-3 staining was recognized by observing the brownish coloration of the immunoreactive cells [38].

The immunoreactivity of caspase-3 was subsequently measured by quantitative morphometric assay of mean area percentage in immuno-stained liver sections. It was measured in five high-power different fields from six rats using "Leica Qwin 500" (Microsystems Imaging Solutions Ltd, Cambridge, United Kingdom) as an image analyzer computer system. Then, data were statistically analyzed.

Transmission electron microscopy (TEM)

Fixing the freshly sliced liver tissues was done by 3 % glutaraldehyde (pH 7.4) in phosphate buffer followed by 2 % osmium tetroxide in phosphate buffer. Tissues were processed in increasing ethanol concentrations before being immersed in araldite resin. Staining of ultrathin liver slices was performed using uranyl acetate saturated in 70 % ethanol and lead citrate [39]. The preparation was performed in the Faculty of Science, Zagazig University and examined using a JEOL transmission electron microscope JEM-100, CX, Japan.

Statistical analysis

Results were presented as mean ± SD by using SPSS program version 26 (SPSS Inc. Chicago, IL, USA). Shapiro-Wilk's test was used to test Quantitative data normality. Normally distributed data was considered if P>0.05. One-way analysis of variance (ANOVA) was used to assign differences in quantitative data among groups of the research, followed by *post hoc* least significant differences (LSD) test. The significance of statistically analyzed data was depicted, when the P-value is less than 0.05.

Results

Effect of fasudil on anthropometric parameters

At the beginning of the study, there were no significant variations in body weight across the groups. When comparing the HFD+T2DM group to the control group, marked body weight gain and significant increases in BMI, AC, and AC/TC ratio were detected at the end of the study duration (after 12 weeks). In contrast to the HFD+T2DM group, rats in the HFD+T2DM+Fasudil group showed significant reductions in all indicators of obesity when compared to the HFD+T2DM group (Table 1).

Effect of fasudil on liver weight and liver index

In compared to the control group, the HFD+T2DM group had a dramatic increase in liver weight and liver index. Conversely, fasudil treatment led to a considerable drop in liver weight and liver index in the HFD+T2DM+Fasudil group relative to HFD+T2DM group (Table 1).

Effect of fasudil on serum glucose, lipid and metabolic profiles

The HFD+T2DM group, showed marked rise in serum glucose, insulin, HOMA-IR, TC, TG, LDL, and hepatic TG levels in addition to significant reduction in HDL compared to normal control group. In the HFD+T2DM+Fasudil group, fasudil treatment significantly lowered serum glucose, insulin, HOMA-IR, TC, TG, LDL, and hepatic TG levels while significantly elevated HDL level compared to the HFD+T2DM group (Table 2).

Effect of fasudil on liver enzymes, albumin, hepatic inflammatory markers

The impact of fasudil on liver function, inflammatory marker alterations, and hepatic TG was evaluated. In comparison to the normal control group, the HFD+T2DM group exhibited a significant rise in the levels of ALT, AST, TNF-α, hs-CRP, and liver TG and significant reduction in the levels of albumin. In the HFD+T2DM+Fasudil group, daily injections of fasudil significantly lowered ALT, AST, TNF-, and CRP levels, but significantly raised albumin levels when compared to the HFD+T2DM group (Table 2).

Effect of fasudil on hepatic oxidant/antioxidant markers

We evaluated the MDA levels as an oxidative stress marker and the antioxidant enzymatic activity of SOD, GST, and GPx levels were evaluated to assess how fasudil influenced markers of hepatic oxidative stress. When comparing the HFD+T2DM group to the normal control group, it was reported that hepatic MDA levels were significantly higher, while SOD, GST, and GPx activities were significantly lower. In HFD+T2DM+Fasudil rats, daily injection of fasudil for 6 weeks drastically improved these alterations (Table 3).

Histopathological results of liver tissue

In the control group, hepatic H&E histopathology revealed normal hepatic architecture, showing a normal hepatocyte grouped around a central vein in the form of cords spaced by blood sinusoids (Fig. 1A). HFD induced non-alcoholic steatohepatitis with marked micro and macro steatosis in hepatocytes (steatosis score 3) with ballooning degeneration and lobular inflammatory infiltrate with the congested dilated central vein in HFD+T2DM group, NASH score from 5 to 6 (Fig. 1B). Moreover, HFD+T2DM+Fasudil group revealed a significant amelioration in hepatic lesions with mildly dilated central veins and partially restoring the normal architecture of the liver where most hepatocytes show normal vesicular nuclei, but still showing mild fatty changes in the form of macrosteatosis in hepatocytes and hydroid degeneration in comparison to HFD+T2DM group (Fig. 1C). Sirius red stained sections were examine and scored for hepatic fibrosis showing strong deposition of coarse collagen fibers around the portal areas extending to few hepatic lobular septa (score 2) in HFD+T2DM group (Fig. 2B) compared to control (Fig. 2A), which showed no fibrosis (score 0) except for fine scarce collagen around some portal areas and central vein. Whereas, HFD+T2DM+Fasudil group revealed marked reduction in collagen deposition around portal areas (Fig. 2C) and central vein (score 1) (Table 4). Furthermore, collagen deposition (mean area %) was significantly (P<0.001) less in HFD+T2DM+Fasudil group compared to HFD+T2DM as showed by the quantitative analysis using Image J software (Fig. 2D).

Caspase-3 immuno- staining

The control group had negligible positive reacted cells (Fig. 3A), according to immunohistochemical staining of liver tissue. The immunoreactivity of other experimental groups to caspase-3 was shown in (Fig. 3B-D) revealing an apparently positive brown cytoplasmic reactivity in a majority of cells in HFD+T2DM group sections (Fig. 3B). Oppositely, the tissue of the HFD+T2DM+Fasudil group, showed just a few scattered positive brown cytoplasmic reactive cells (Fig. 3C). The % area of caspase-3 immuno-expression in the HFD+T2DM group, demonstrated a considerable increased expression of caspase-3 relative to the control rats. These effects in the HFD+T2DM+Fasudil group show a significant decrease confirming the microscopic observations as illustrated in (Fig. 3D), (Table 5).

Transmission electron microscopy examination

Normal hepatic structure was observed in

TEM examined liver sections of the control group (hepatocytes revealed typical nucleoplasm with spherical nuclei surrounded by an apparent nuclear envelop with fine granular chromatin). The cytoplasm showed mitochondria, rough endoplasmic reticulum, glycogen inclusions (Fig. 4A, B). In HFD+T2DM, abnormal hepatocytes with large aberrant lipid droplets, glycogen inclusions depletion, and swollen mitochondria were detected in addition to reduced junctional complexes in the cytoplasm of hepatocytes, and wide sinusoidal spaces (Fig. 5A, B, C, D). However, as compared to the HFD+T2DM group, the HFD+T2DM+Fasudil group demonstrated improvement in the context of fewer lipid droplets, normal nucleoplasm in the hepatocytes, with spherical nuclei surrounded by an evident nuclear envelop and fine granular chromatin. Mitochondria, rough endoplasmic reticulum, glycogen inclusions reappeared, and Mallory bodies were all seen in the cytoplasm signifying a change in hepatocyte morphology with fasudil treatment (Fig. 6).

Table 1. Anthropometric parameters, liver weight and liver index in all studied groups.

Parameters	Control	HFD+T2DM	HFD+T2DM+Fasudil
Initial body weight (g)	161.11 ± 13.33	163.32 ± 5.63	160.62 ± 9.61
Final body weight (g)	202.32 ± 17.81	$329.21 \pm 13.12^{a***}$	$284.30 \pm 26.62^{a***,\ b**}$
Final BMI (g/cm^2)	0.57 ± 0.06	$0.86 \pm 0.08^{a***}$	$0.66 \pm 0.09^{a**,\ b**}$
AC (cm)	16.75 ± 1.10	$22.03 \pm 1.67^{a***}$	$20.6 \pm 1.15^{a***}$
AC/TC ratio	1.07 ± 0.02	$1.16 \pm 0.05^{a***}$	$1.11 \pm 0.03^{a*,\ b*}$
Liver weight (g)	6.08 ± 0.87	$12.85 \pm 1.74^{a***}$	$9.77 \pm 1.53^{a***,\ b**}$
Liver index (%)	2.99 ± 0.21	$4.14 \pm 0.23^{a***}$	$3.54 \pm 0.20^{a***,\ b**}$

Data are expressed as mean ± SD. P value by one-way ANOVA, followed by *post hoc* test "LSD"; [a] vs. Control group; [b] vs. HFD+T2DM group. P<0.05 is considered statistically significant. * P<0.05, ** P<0.01, *** P<0.001. Abbreviations: BMI: body mass index; AC: abdominal circumference; TC: thoracic circumference.

Table 2. Serum biochemical parameters and TG in liver homogenate in all studied groups.

Parameters	Control	HFD+T2DM	HFD+T2DM+Fasudil
Glucose (mmol/l)	4.79 ± 0.62	$11.18 \pm 1.76^{a***}$	$9.41 \pm 1.02^{a***,\ b*}$
Insulin (pmol/l)	1399.31 ± 220.42	$175.35 \pm 34.24^{a***}$	$132.15 \pm 27.57^{a**,\ b*}$
HOMA-IR index	2.47 ± 0.83	$12.85 \pm 4.27^{a***}$	$8.11 \pm 2.44^{a**,\ b**}$
Cholesterol (mmol/l)	2.91 ± 0.22	$4.73 \pm 1.12^{a***}$	$4.00 \pm 0.42^{a**}$
Triglycerides (mmol/l)	0.84 ± 0.16	$1.60 \pm 0.33^{a***}$	$1.21 \pm 0.33^{a*,\ b*}$
HDL-c (mmol/l)	1.25 ± 0.23	$0.61 \pm 0.22^{a***}$	$0.87 \pm 0.17^{a**,\ b*}$
LDL-c (mmol/l)	1.22 ± 0.25	$2.42 \pm 0.55^{a***}$	$1.81 \pm 0.50^{a*,\ b*}$
Albumin (μmol/l)	568.76 ± 48.15	$448.39 \pm 55.67^{a***}$	$511.59 \pm 31.60^{a*,\ b*}$
ALT (μkat/l)	0.69 ± 0.07	$1.49 \pm 0.20^{a***}$	$0.94 \pm 0.18^{a**,\ b***}$
AST (μkat/l)	1.34 ± 0.15	$2.00 \pm 0.20^{a***}$	$1.59 \pm 0.25^{a*,\ b**}$
TNF-α (pg/ml)	15.25 ± 3.81	$44.16 \pm 9.41^{a***}$	$32.83 \pm 8.54^{a***,\ b*}$
hs-CRP (nmol/l)	0.42 ± 0.17	$1.11 \pm 0.35^{a***}$	$0.76 \pm 0.22^{a*,\ b*}$
Hepatic TG (mg/g)	8.86 ± 0.69	15.29 ± 0.95	12.00 ± 0.81

Data are expressed as mean ± SD. P value by one-way ANOVA, followed by *post hoc* test "LSD"; [a] vs. Control group; [b] vs. HFD+T2DM group. P<0.05 is considered statistically significant. * P<0.05, ** P<0.01, *** P<0.001. Abbreviations: HOMA-IR index: Homeostatic Model Assessment-Insulin Resistance index; HDL-c: high density lipoprotein-cholesterol; LDL-c: low density lipoprotein-cholesterol; ALT: Alanine aminotransferase, AST: Aspartate aminotransferase; TNF-α: Tumor necrosis factor α; CRP: C-reactive protein; TG: triglyceride.

Table 3. Oxidative stress markers in all studied groups.

Parameters	Control	HFD+T2DM	HFD+T2DM+Fasudil
MDA (nmol/g protein)	2.04 ± 0.35	4.13 ± 1.28[a]**	3.13 ± 1.06[a]*
SOD (U/mg protein)	74.52 ± 16.16	25.00 ± 10.43[a]***	48.8 ± 15.53[a]**, [b]*
GST activity (U/mg protein)	11.88 ± 1.85	5.58 ± 2.03[a]***	9.25 ± 1.14[a]*, [b]**
GPx activity (U/mg protein)	1.88 ± 0.14	0.52 ± 0.15[a]***	1.33 ± 0.12[a]***, [b]***

Data are expressed as mean ± SD. P value by one-way ANOVA, followed by *post hoc* test "LSD"; [a] vs. Control group; [b] vs. HFD+T2DM group. P<0.05 is considered statistically significant. * P<0.05, ** P<0.01, *** P<0.001. Abbreviations: MDA: malondialdehyde; SOD: superoxide dismutase; GST: Glutathione S-transferase; GPx: Glutathione Peroxidase.

Table 4. Histopathological scoring of liver injury induced by HFD.

Parameter	Control	HFD+T2DM	HFD+T2DM+Fasudil
NAS	0 ± 0	6.08 ± 1.42[a]***	2.33 ± 0.82[a]***, [b]***

Data are expressed as mean ± SD. P value by one-way ANOVA, followed by *post hoc* test "LSD"; [a] vs. Control group; [b] vs. HFD+T2DM group. P<0.05 is considered statistically significant. *** P<0.001. Abbreviations NAS: NAFLD activity scoring.

Table 5. Immunohistochemical expression of caspase -3 in the three studied groups.

Parameter	Control	HFD+T2DM	HFD+T2DM+Fasudil
Caspase-3 expression	0.78 ± 0.18	2.67 ± 0.79[a]***	1.83 ± 0.46[a]**, [b]*

Data are expressed as mean ± SD. P value by one-way ANOVA, followed by *post hoc* test "LSD"; [a] vs. Control group; [b] vs. HFD+T2DM group. P<0.05 is considered statistically significant. * P<0.05, ** P<0.01, *** P<0.001.
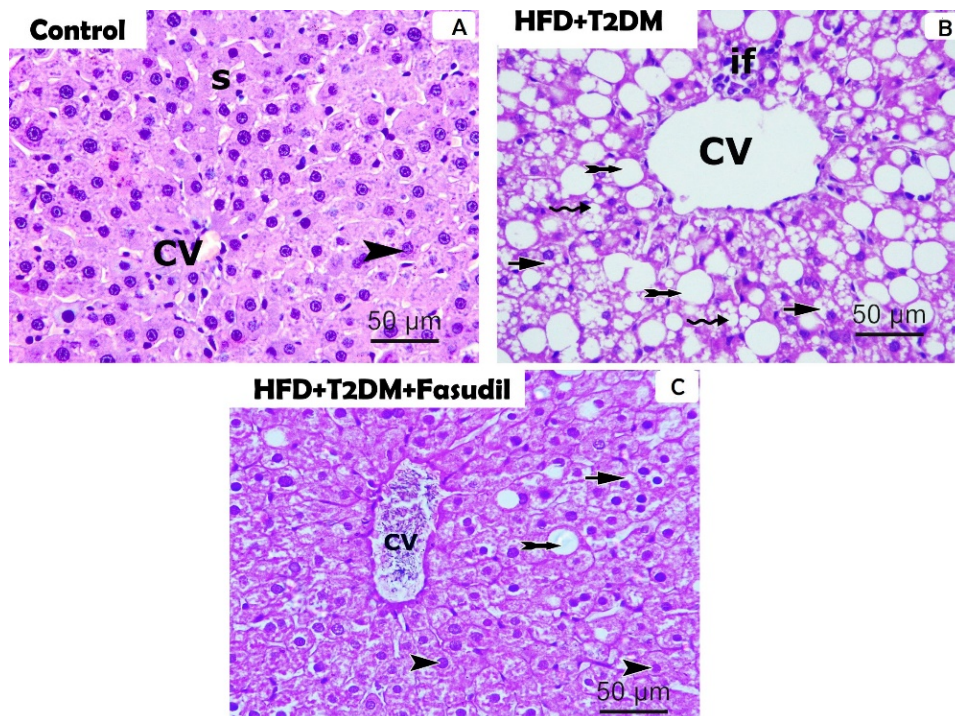
Fig. 1. representative photomicrograph of H&E stain of liver tissue of normal control group (**A**): showing central vein (cv) surrounded with normal hepatocytes (arrow head) arranged in cords and separated by blood sinusoids (s); HFD+T2DM group (**B**): liver tissue showing dilated central veins (CV), NASH with marked micro (wavy arrow) and macro (bifid arrow) -steatosis in hepatocytes with ballooning degeneration (short arrow) along with inflammatory cellular infiltration (if); HFD+T2DM+Fasudil group (**C**): showing mildly dilated central veins (cv) and partially restoring the normal architecture of the liver where most hepatocytes show normal vesicular nuclei (arrow head), but still showing mild fatty changes in the form of macrosteatosis in hepatocytes (bifid arrow) and hydrobic degeneration (short arrow) (H&E ×400).
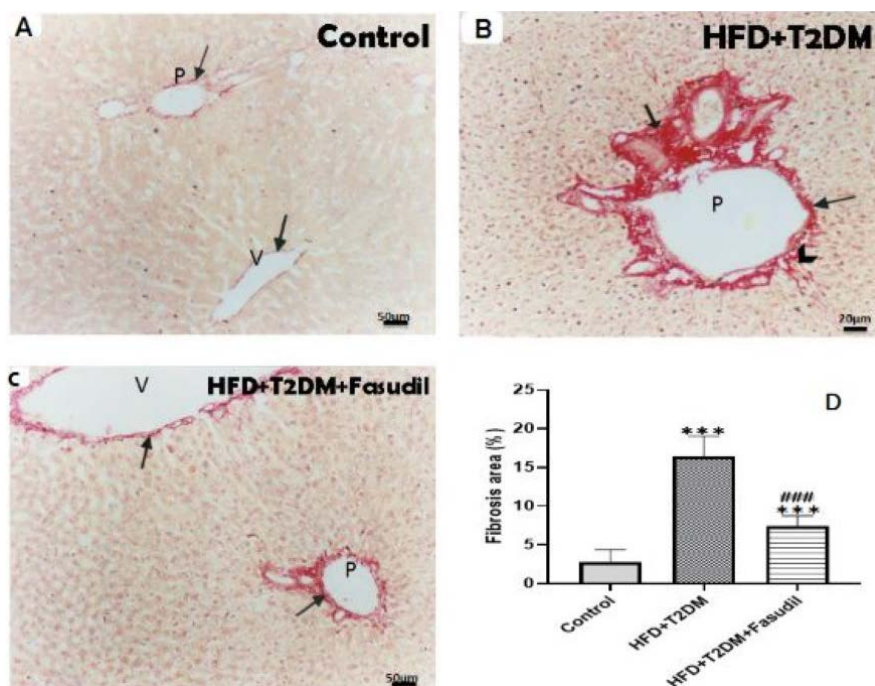
Fig. 2. Representative image of Sirius red stained liver tissue collected from all rats' groups; (**A**) Control (**B**) HFD+T2DM group (**C**) HFD+T2DM+Fasudil group. Arrows in (A) point to the fine collagen deposition in the portal area (P) and surrounding the central vein (V), arrows and arrow head in (B) point to the heavy collagen deposition encircling the portal region (P) and extending in the septa. Whereas, arrows in (C) point to the fine collagen deposition around both portal area (P) and central vein (V). Magnification, ×200. (**D**) Represents a quantitative analysis of liver fibrosis determined by % collagen deposition calculation from Sirius red stain. Data are displayed as mean ± SD. *** P<0.001 vs. control group and ### P<0.001 vs. HFD+T2DM group.
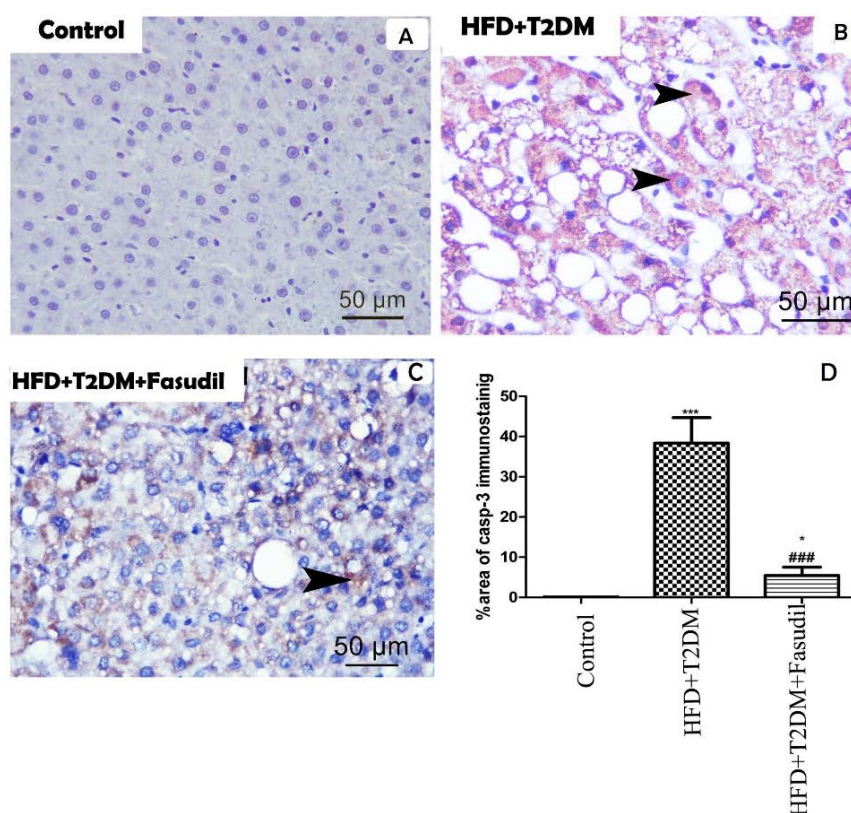

Fig. 3. Representative image of immunohistochemical staining of liver sections with anti-caspase-3 antibody from various studied groups (**A**) Control (**B**) HFD+T2DM group (**C**) HFD+T2DM+Fasudil group. Arrowhead points to the brown coloration of the immuno-positive cells. (**D**) Histogram shows the % area of immuno- positive cells from the various experimental groups. HFD+T2DM group showed significant increase in caspase-3 immunostaining compared to other groups. HFD+T2DM+Fasudil group revealed weakly positive immunostaining.
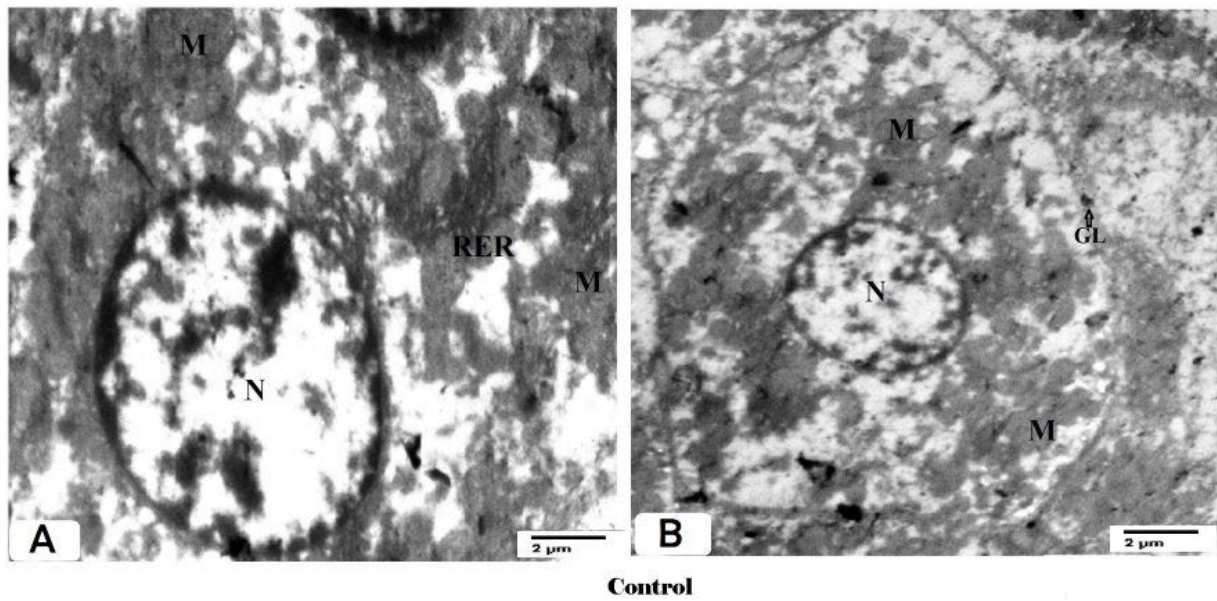
Control

Fig. 4. TEM representative of the liver tissue of normal control rats. (**A**) Revealed normal hepatocytes as well as normal sinusoids with no abnormal features. The hepatocytes showed normal nucleoplasm with round nuclei surrounded by obvious nuclear envelop with fine granular chromatin. The cytoplasm showed mitochondria (M), rough endoplasmic reticulum (RER). (**B**) Revealed normal hepatocytes with normal nucleoplasm with round nuclei and nuclear envelop. The cytoplasm showed mitochondria (M), glycogen inclusions (GL).
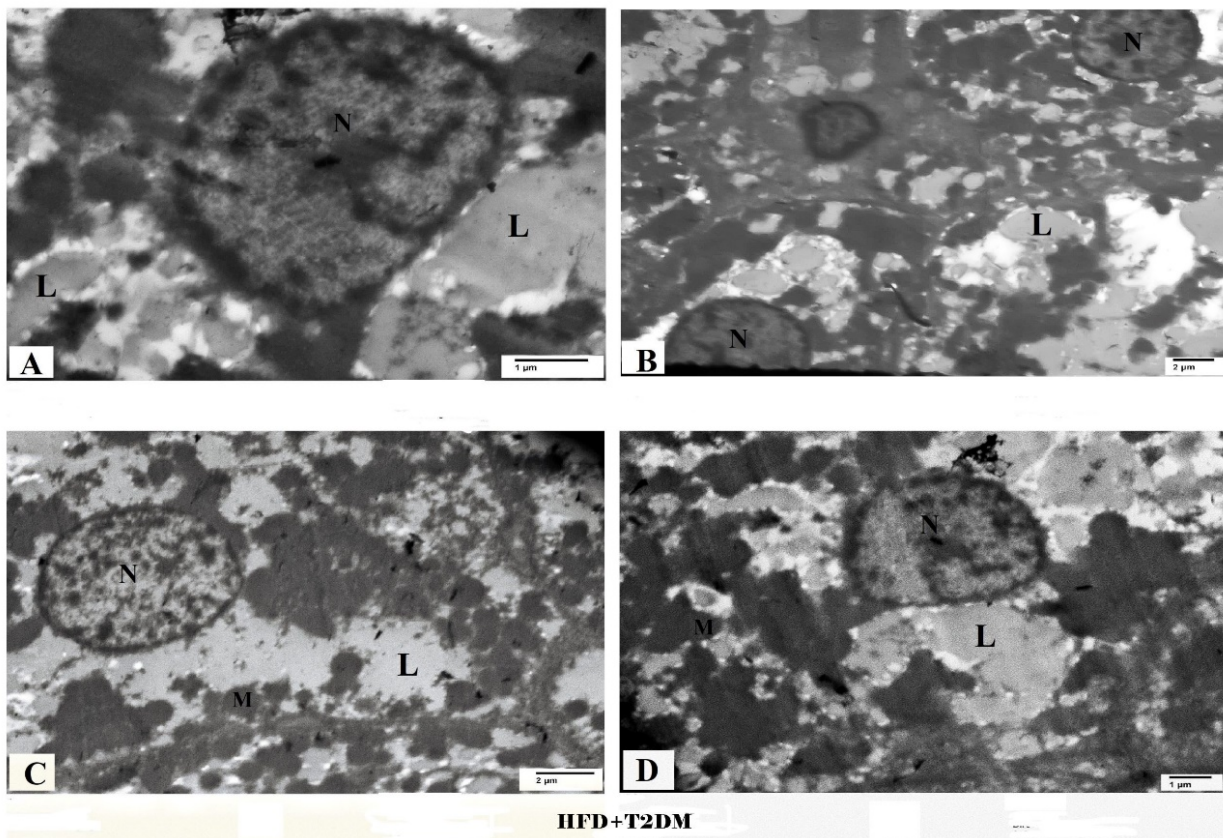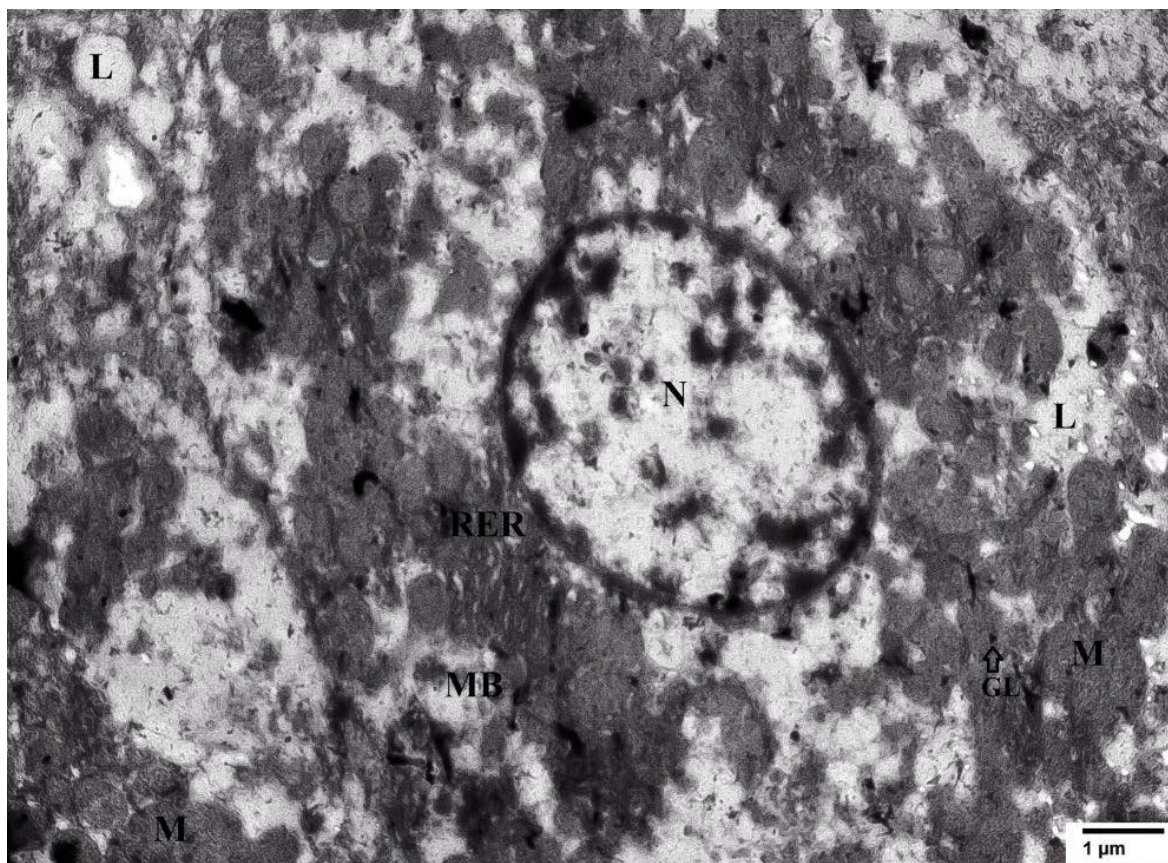

HFD+T2DM

Fig. 5. TEM examination of the liver tissue of HFD+T2DM group. (**A**) Showed abnormal hepatocytes with wide sinusoids, marked fat droplets infiltration (L) with glycogen inclusions depletion. (**B**) Abnormal hepatocytes with wide sinusoids, marked fat droplets infiltration (L). (**C**) Abnormal hepatocytes with wide sinusoids swollen mitochondria (M), marked fat droplets infiltration (L) with infrequent glycogen inclusions. (**D**) The abnormal hepatocytes with abnormal nuclear chromatin distribution (N), significant fat droplets infiltration (L).

HFD+T2DM+Fasudil

Fig. 6. TEM examination of the liver tissue of HFD+T2DM+Fasudil group, revealed improved hepatocytes appearance. The hepatocytes showed normal nucleoplasm with round nuclei surrounded by obvious nuclear envelop with fine granular chromatin. The cytoplasm showed mitochondria (M), rough endoplasmic reticulum (RER), reappearance of glycogen inclusions (GL), and Mallory body (MB).

Discussion

Several studies [40,42] have proven a link between NAFLD, type 2 diabetic patients, and obesity. NAFLD poses a serious threat because it has been identified as a trigger for subacute liver failure, cirrhosis, and hepatoma [43]. Furthermore, there were metabolic problems associated with it, such as hyperglycemia, insulin resistance, and hyperlipidemias [44], which were linked to inflammation and oxidative stress [45].

The rat model of NAFLD was effectively constructed in the current study. Insulin resistance was created from a single STZ injection (30 mg/kg) to generate an evident hyperglycemia, followed by the HFD feeding regimen [46].

The metabolic syndrome induced by obesity was found to be related to Rho-associated coiled-coil-containing kinase (ROCK) [47,48], a serine/threonine protein kinase identified as a guanosine triphosphate (GTP)-Rho-binding protein, which induce insulin resistance through influencing the insulin receptor

substrate-1 (IRS-1) phosphorylation [49]. Fasudil was documented as an inhibitor of the ROCK pathway, which interfere with both ROCK1 and ROCK2 kinase activity [50]. Therefore, we built our hypothesis upon the previously mentioned documentations and investigated the impact of fasudil on NAFLD in type 2 diabetic rats. Figure 7 summarizes the anti-NAFLD mechanistic activity of fasudil.

The model group (HFD+T2DM) showed marked body weight gain, increased BMI, and AC/TC ratio in relation to control group, as previously reported by Gaballah *et al.* [51]. Moreover, histopathological examination of extracted liver tissue from rats of HFD+T2DM group showed the typical picture of NAFLD-related initial portal fibrosis. Figure 1B, which was discussed by earlier studies [52,53], in addition to the microstructural changes revealed by TEM pictures showing early stage of mitochondrial degeneration (Fig. 5A-D). Also, there was an accompanying hyperglycemia, hyperinsulinemia, dyslipidemia, and deterioration of hepatic functions with elevation of

hepatic oxidative stress and proapoptotic markers expression. Whereas, fasudil-treated group showed amelioration of all hepatic structural (Fig. 1C, 6) and functional alterations together with improved metabolic

changes primarily insulin resistance and glucose dysregulation, which are greatly involved in T2DM and NAFLD [54,55].
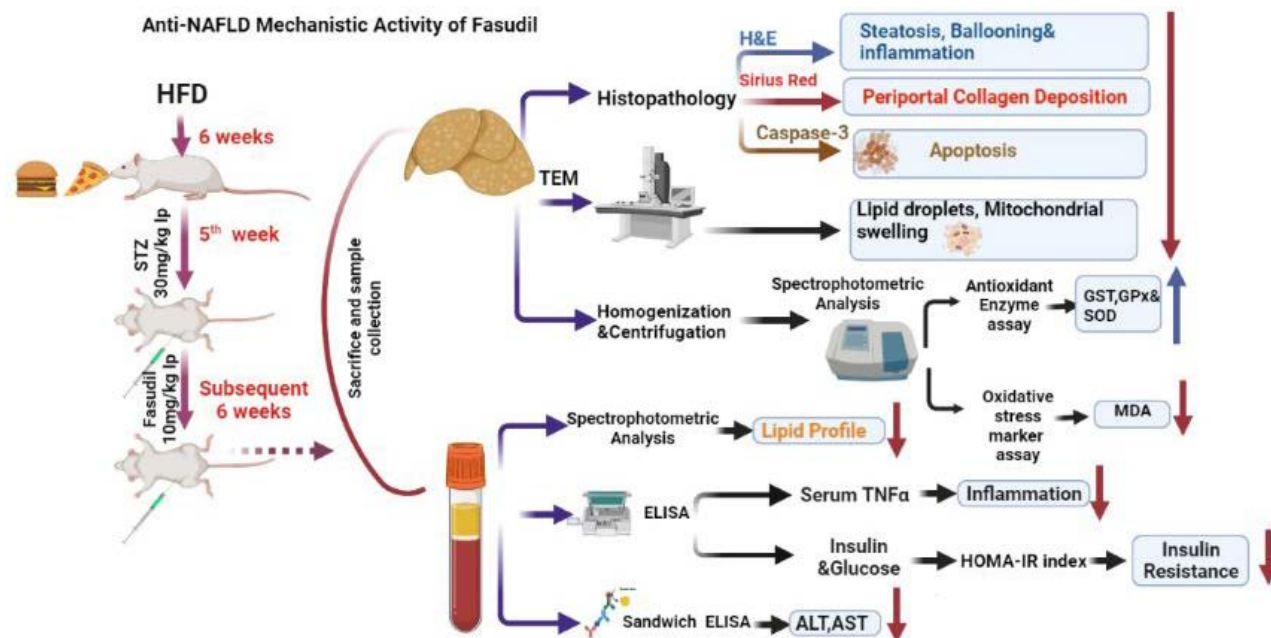

Fig. 7. A summarized graph of the anti-NAFLD mechanistic activity of fasudil.

The improved structural and functional deteriorations of liver with fasudil treatment was supported by Kuroda *et al.* [56] who reported enhanced hepatic blood flow in rat steatotic livers after hepatic ischemia-reperfusion injury with the use of Rho-kinase inhibitors, which induced direct relaxation of hepatic stellate cells concomitant with nitric oxide synthase activation in sinusoidal endothelial cells, and suppression of neutrophil infiltration [57,58]. Moreover, fasudil administration reduced liver fibrosis in type 2 diabetics by suppressing transforming growth factor-β1 (TGFβ1)/connective tissue growth factor (CTGF) pathway and α-smooth muscle actin (α-SMA) expression, according to a prior study [12], which is consistent with our findings of reduced collagen deposition around portal areas and central vein in Sirius red stained liver sections.

The correlation between the ROCK activity, T2DM, obesity, fatty liver, and insulin resistance was reported after observing an elevated hepatic ROCK receptors expression concomitant with marked hepatic damage in obese diabetic animal models [9]. The Rho kinase inhibition impact on obesity and insulin resistance was attributed to its impact in adjusting the obese rats' uncoupling protein 1 (UCP-1) levels [59], which

consequently reflects on the AMPK [60] resulting in enhanced insulin sensitivity and body weight reduction [61]. This is in agreement with our observations in HFD+T2DM+Fasudil group, which showed improvements in glucose dysregulation, insulin resistance, and body weight loss.

NAFLD was linked with high total cholesterol, TG, LDL-c, and low HDL-c serum levels as previously reported [37,62], all of which improved with fasudil treatment in the current study. This improvement can be explained by controlled fatty acid oxidation, and mitochondrial energy production [61] through peroxisome proliferator-activated receptor (PPAR)-α activation [63], which modulates dyslipidemia and arrests the NAFLD progression in obese diabetic rats.

Increased serum TNF-α protein, IL-6, IL-1β, and CRP levels have been assigned as contributory factors of NAFLD development with prolonged HFD consumption [64] and linked to activation of Kupffer cells in the liver [65]. Many studies have reported ROCK Inhibitors as anti-inflammatory [66,67] emphasizing their role against TNF-α induced inflammation in diabetes [68]. The mitigating effect of fasudil on serum TNF-α, IL-6, and CRP levels in HFD-fed rats is mediated by ROCK

pathway inhibition [69] distorting the axis of TNF-α/NADPH oxidase-dependent reactive oxygen species (ROS) generation [68], this is in consistent with our observations, which showed a significantly suppressed activity of hepatic SOD and GST, and higher MDA levels concomitant with lower hepatic inflammatory markers expression.

NAFLD has been linked to increased mitochondrial ROS levels and inhibited ROS detoxifying mechanisms in different studies, which were carried *in vitro* or *in vivo* [70-72]. This mitochondrial dysfunction had significant role in emergence of insulin resistance and T2DM as reported previously by Urbanova *et al.* [73]. The potential antioxidant effect of fasudil is related nuclear translocation of nuclear factor-like 2 activation [74]. Moreover, using fasudil, improved mitochondrial structure in HFD/STZ diabetic rats with subsequent attenuation of oxidative stress [75], which is consistent with our findings regarding improved mitochondrial architecture in hepatocytes as shown by transmission electron microscopy.

Hepatocellular apoptosis and excessive lipid buildup were discovered to have a significant link, with free fatty acids being the primary inducers of "lipoapoptosis" [76]. The level of cytochrome c in mitochondria has been distinguished as the most striking feature of NAFLD in majority of animal models, and was linked to the disease severity [77]. Accordingly, fasudil effect on the caspase-3 hepatic expression was analyzed showing a marked attenuation in HFD+T2DM+Fasudil group compared to HFD+T2DM group. This is consistent with findings of Thorlacius *et al.* [78], who reported reduction of hepatic levels of caspase-3 with fasudil in septic liver injury due to direct inhibition hepatic infiltration of leukocytes and TNF-α production. Furthermore, Ikeda *et al.* [79] demonstrated that Rho-

kinase inhibitors reduce apoptosis in cultured hepatocytes by lowering the caspase-3 activity and stimulating the Akt (protein kinase B), which disrupts the phosphatidylinositol 3-kinase (PI3-kinase)/Akt pathway.

Our findings revealed that fasudil treatment resulted in a noteworthy decrement in the hepatic lesions, as well as a partial restoration of the liver's natural architecture and function. Our findings further show that fasudil may have a hepatoprotective impact in the liver by preserving hepatic mitochondria and having an anti-apoptotic effect. This new pathway could be added to existing ones such as anti-inflammatory, anti-oxidative, and insulin resistance reduction.

Conclusions

The present study emphasizes the beneficial ameliorating effect of fasudil on NAFLD and the underlying mechanisms including improved dyslipidemia, attenuated oxidative stress, downregulated inflammation, improved mitochondrial architecture, and apoptosis. Taken together, these data shed light on fasudil use as a potential promising protective agent against liver injury in HFD fed rats and other therapeutic purposes.

Conflict of Interest
There is no conflict of interest.

Acknowledgements

References

1. Giacco F, Brownlee M, Schmidt AM. Oxidative stress and diabetic complications. Circ Res 2010;107:1058-1070. https://doi.org/10.1161/CIRCRESAHA.110.223545
2. Adams LA, Anstee QM, Tilg H, Targher G. Non-alcoholic fatty liver disease and its relationship with cardiovascular disease and other extrahepatic diseases. Gut 2017;66:1138-1153. https://doi.org/10.1136/gutjnl-2017-313884
3. Li L, Lou X, Zhang K, Yu F, Zhao Y, Jiang P. Hydrochloride fasudil attenuates brain injury in ICH rats. Transl Neurosci 2020;11:75-86. https://doi.org/10.1515/tnsci-2020-0100
4. Ramakrishna G, Rastogi A, Trehanpati N, Sen B, Khosla R, Sarin SK. From cirrhosis to hepatocellular carcinoma: new molecular insights on inflammation and cellular senescence. Liver Cancer 2013;2:367-383. https://doi.org/10.1159/000343852

5.   Akshintala D, Chugh R, Amer F, Cusi K. Nonalcoholic fatty liver disease: the overlooked complication of type 2 diabetes. Endotext [Internet] 2019.

6.   Schuppan D, Schattenberg JM. Non-alcoholic steatohepatitis: pathogenesis and novel therapeutic approaches. J Gastroenterol Hepatol 2013;28:68-76. https://doi.org/10.1111/jgh.12212

7.   Matsuzaka T, Shimano H. New perspective on type 2 diabetes, dyslipidemia and non-alcoholic fatty liver disease. J Diabetes Investig 2020;11:532-534. https://doi.org/10.1111/jdi.13258

8.   Shimokawa H, Takeshita A. Rho-kinase is an important therapeutic target in cardiovascular medicine. Arterioscler Thromb Vasc Biol 2005;25:1767-1775. https://doi.org/10.1161/01.ATV.0000176193.83629.c8

9.   Huang H, Lee S-H, Sousa-Lima I, Kim SS, Hwang WM, Dagon Y, Yang W-M, ET AL. Rho-kinase/AMPK axis regulates hepatic lipogenesis during overnutrition. J Clin Invest 2018;128:5335-5350. https://doi.org/10.1172/JCI63562

10.   Garcia D, Shaw RJ. AMPK: mechanisms of cellular energy sensing and restoration of metabolic balance. Mol Cell 2017;66:789-800. https://doi.org/10.1016/j.molcel.2017.05.032

11.   Komers R. Rho kinase inhibition in diabetic kidney disease. Br J Clin Pharmacol 2013;76:551-559. https://doi.org/10.1111/bcp.12196

12.   Zhou H, Fang C, Zhang L, Deng Y, Wang M, Meng F. Fasudil hydrochloride hydrate, a Rho-kinase inhibitor, ameliorates hepatic fibrosis in rats with type 2 diabetes. Chin Med J 2014;127:225-231. https://doi:10.3760/cma.j.issn.0366-6999.20131917

13.   Musabayane C, Mahlalela N, Shode F, Ojewole J. Effects of Syzygium cordatum (Hochst.)[Myrtaceae] leaf extract on plasma glucose and hepatic glycogen in streptozotocin-induced diabetic rats. J Ethnopharmacol 2005;97(3):485-490. https://doi.org/10.1016/j.jep.2004.12.005

14.   Nascimento AF, Sugizaki MM, Leopoldo AS, Lima-Leopoldo AP, Nogueira CR, Novelli ELB, Padovani CR, Cicogna AC. Misclassification probability as obese or lean in hypercaloric and normocaloric diet. Biol Res 2008;41:253-259. https://doi.org/10.4067/S0716-97602008000300002

15.   Novelli E, Diniz Y, Galhardi C, Ebaid G, Rodrigues H, Mani F, Fernandes AAH, ET AL. Anthropometrical parameters and markers of obesity in rats. Lab Anim 2007;41:111-119. https://doi.org/10.1258/002367707779399518

16.   Alghannam MA, Khalefa AA, Alaleem D, Ahmad AA. Plasma vaspin levels in relation to diet induced metabolic disturbance in rats. Int J Diabetes Res 2013;2:112-122. https://doi.org/10.5923/j.diabetes.20130206.04

17.   Nishizawa H, Shimomura I, Kishida K, Maeda N, Kuriyama H, Nagaretani H, Matsuda M, ET AL. Androgens decrease plasma adiponectin, an insulin-sensitizing adipocyte-derived protein. Diabetes 2002;51:2734-2741. https://doi.org/10.2337/diabetes.51.9.2734

18.   Ebrahim HA, Alzamil NM, Al-Ani B, Haidara MA, Kamar SS, Dawood AF. Suppression of knee joint osteoarthritis induced secondary to type 2 diabetes mellitus in rats by resveratrol: role of glycated haemoglobin and hyperlipidaemia and biomarkers of inflammation and oxidative stress. Arch Physiol Biochem 2020:1-8. https://doi.org/10.1080/13813455.2020.1771378

19.   Sabir U, Irfan HM, Alamgeer AU, Althobaiti YS, Asim MH. Reduction of hepatic steatosis, oxidative stress, inflammation, ballooning and insulin resistance after therapy with safranal in NAFLD animal model: a new approach. J Inflamm Res 2022;15:1293. https://doi.org/10.2147/JIR.S354878

20.   Bonora E, Targher G, Alberiche M, Bonadonna RC, Saggiani F, Zenere MB, Monauni T, Muggeo M. Homeostasis model assessment closely mirrors the glucose clamp technique in the assessment of insulin sensitivity: studies in subjects with various degrees of glucose tolerance and insulin sensitivity. Diabetes Care 2000;23:57-63. https://doi.org/10.2337/diacare.23.1.57

21.   Fossati P, Prencipe L. Serum triglycerides determined colorimetrically with an enzyme that produces hydrogen peroxide. Clin Chem 1982;28:2077-2080. https://doi.org/10.1093/clinchem/28.10.2077

22.   Nauck M, Marz W, Jarausch J, Cobbaert C, Sagers A, Bernard D, Delanghe J, ET AL. Multicenter evaluation of a homogeneous assay for HDL-cholesterol without sample pretreatment. Clin Chem 1997;43:1622-1629. https://doi.org/10.1093/clinchem/43.9.1622

23. Friedewald WT, Levy RI, Fredrickson DS. Estimation of the concentration of low-density lipoprotein cholesterol in plasma, without use of the preparative ultracentrifuge. Clin Chem 1972;18:499-502. https://doi.org/10.1093/clinchem/18.6.499

24. Foster LB, Dunn RT. Stable reagents for determination of serum triglycerides by a colorimetric Hantzsch condensation method. Clin Chem 1973;19:338-340.

25. Folch J, Lees M, Sloane Stanley GH. A simple method for the isolation and purification of total lipids from animal tissues. J Biol Chem 1957;226:497-509. https://doi.org/10.1016/S0021-9258(18)64849-5

26. Vassault A. Lactate dehydrogenase: UV-method with pyruvate and NADH. Methods Enzym Anal 1984;3:118-126.

27. Wack RF, Warmolts DI. Fish medicine. JSTOR 1994;2:548-549. https://doi.org/10.2307/1447015

28. Song L, Qu D, Zhang Q, Jiang J, Zhou H, Jiang R, Li Y, ET AL. Phytosterol esters attenuate hepatic steatosis in rats with non-alcoholic fatty liver disease rats fed a high-fat diet. Sci Rep 2017;7:41604. https://doi.org/10.1038/srep41604

29. Varshey R, Kale R. Effect of calmodulin antagonist on radiation induced lipid peroxidation in microsome. Int J Rad Biol 1990;58:733-743. https://doi.org/10.1080/09553009014552121

30. Misra HP, Fridovich I. The role of superoxide anion in the autoxidation of epinephrine and a simple assay for superoxide dismutase. J Biol Chem 1972;247:3170-3175. https://doi.org/10.1016/S0021-9258(19)45228-9

31. Rajurkar RB, Khan ZH, Gujar GT. Studies on levels of glutathione S-transferase, its isolation and purification from Helicoverpa armigera. Curr Sci Ind 2003;85:1355-1360.

32. Paglia DE, Valentine WN. Studies on the quantitative and qualitative characterization of erythrocyte glutathione peroxidase. J Lab Clin Med 1967;70:158-169.

33. Altunkaynak Z. Effects of high fat diet induced obesity on female rat livers (a histochemical study). Eur J Gen Med 2005;2:100-109. https://doi.org/10.29333/ejgm/82319

34. Kleiner D, Brunt E, Van Natta M, Behling C, Contos M, Cummings O, Ferrell LD, ET AL. Design and validation of a histological scoring system for nonalcoholic fatty liver disease. Hepatology 2005;41:1313-1321. https://doi.org/10.1002/hep.20701

35. Zhao C-Y, Jiang L-L, Li L, Deng Z-J, Liang B-L, Li J-M. Peroxisome proliferator activated receptor-γ in pathogenesis of experimental fatty liver disease. World J Gastroenterol 2004;10:1329. https://doi.org/10.3748/wjg.v10.i9.1329

36. Mohamed HE, Elswefy SE, Rashed LA, Younis NN, Shaheen MA, Ghanim AM. Bone marrow-derived mesenchymal stem cells effectively regenerate fibrotic liver in bile duct ligation rat model. Exp Biol Med 2016;241:581-591. https://doi.org/10.1177/1535370215627219

37. El-Sherbiny M, Eldosoky M, El-Shafey M, Othman G, Elkattawy HA, Bedir T, Elsherbiny NM. Vitamin D nanoemulsion enhances hepatoprotective effect of conventional vitamin D in rats fed with a high-fat diet. Chem Biol Interact 2018;288:65-75. https://doi.org/10.1016/j.cbi.2018.04.010

38. Dozic B, Glumac S, Boricic N, Dozic M, Anicic B, Boricic I. Immunohistochemical expression of caspases 9 and 3 in adenoid cystic carcinoma of salivary glands and association with clinicopathological parameters. J BUON 2016;21:152-160.

39. Woods AE, Stirling JW. Transmission electron microscopy. In: *Bancroft's Theory and Practice of Histological Techniques*. Kim Suvarna S, Layton C, Bancroft JD (eds), Science Direct, 2018, pp 434-475. https://doi.org/10.1016/B978-0-7020-6864-5.00021-9

40. Harris EH. Elevated liver function tests in type 2 diabetes. Clin Diabetes 2005;23:115-119. https://doi.org/10.2337/diaclin.23.3.115

41. Ma Z, Chu L, Liu H, Wang W, Li J, Yao W, Yi J, Gao Y. Beneficial effects of paeoniflorin on non-alcoholic fatty liver disease induced by high-fat diet in rats. Sci Rep 2017;7:44819. https://doi.org/10.1038/srep44819

42. Toriniwa Y, Muramatsu M, Ishii Y, Riya E, Miyajima K, Ohshida S, Kitatani K, ET AL. Pathophysiological characteristics of non-alcoholic steatohepatitis-like changes in cholesterol-loaded type 2 diabetic rats. Physiol Res 2018;67:601-612. https://doi.org/10.33549/physiolres.933784

43. Batirel S, Bozaykut P, Altundag EM, Ozer NK, Mantzoros CS. The effect of irisin on antioxidant system in liver. Free Radic Biol Med 2014;75(Suppl 1):S16. https://doi.org/10.1016/j.freeradbiomed.2014.10.592

44. Fotbolcu H, Zorlu E. Nonalcoholic fatty liver disease as a multi-systemic disease. World J Gastroenterol 2016;22:4079. https://doi.org/10.3748/wjg.v22.i16.4079

45. Wree A, Broderick L, Canbay A, Hoffman HM, Feldstein AE. From NAFLD to NASH to cirrhosis-new insights into disease mechanisms. Nat Rev Gastroenterol Hepatol 2013;10:627-636. https://doi.org/10.1038/nrgastro.2013.149

46. Jiang X, Ma H, Wang Y, Liu Y. Early life factors and type 2 diabetes mellitus. J Diabetes Res 2013;2013:485082. https://doi.org/10.1155/2013/485082

47. Kikuchi Y, Yamada M, Imakiire T, Kushiyama T, Higashi K, Hyodo N, Yamamoto K, ET AL. A Rho-kinase inhibitor, fasudil, prevents development of diabetes and nephropathy in insulin-resistant diabetic rats. J Endocrinol 2007;192:595-603. https://doi.org/10.1677/JOE-06-0045

48. Liu P-Y, Chen J-H, Lin L-J, Liao JK. Increased Rho kinase activity in a Taiwanese population with metabolic syndrome. J Am Coll Cardiol 2007;49:1619-1624. https://doi.org/10.1016/j.jacc.2006.12.043

49. Tabur S, Oztuzcu S, Oguz E, Korkmaz H, Eroglu S, Ozkaya M, Demiryürek AT. Association of Rho/Rho-kinase gene polymorphisms and expressions with obesity-related metabolic syndrome. Eur Rev Med Pharmacol Sci 2015;19:1680-1688.

50. Ono-Saito N, Niki I, Hidaka H. H-series protein kinase inhibitors and potential clinical applications. Pharmacol Ther 1999;82:123-131. https://doi.org/10.1016/S0163-7258(98)00070-9

51. Gaballah HH, El-Horany HE, Helal DS. Mitigative effects of the bioactive flavonol fisetin on high-fat/high-sucrose induced nonalcoholic fatty liver disease in rats. J Cell Biochem 2019;120:12762-12774. https://doi.org/10.1002/jcb.28544

52. Ibrahim RH, Fathy MA. Sexual dimorphism in serum kisspeptin level in experimentally induced non alcoholic fatty liver disease in adult albino rats. Am J Biomed Sci 2018;10:115-128. https://doi.org/10.5099/aj180200115

53. Chien M-Y, Ku Y-H, Chang J-M, Yang C-M, Chen C-H. Effects of herbal mixture extracts on obesity in rats fed a high-fat diet. J Food Drug Anal 2016;24:594-601. https://doi.org/10.1016/j.jfda.2016.01.012

54. Ideta T, Shirakami Y, Miyazaki T, Kochi T, Sakai H, Moriwaki H, Shimizu M. The dipeptidyl peptidase-4 inhibitor teneligliptin attenuates hepatic lipogenesis via AMPK activation in non-alcoholic fatty liver disease model mice. Int J Mol Sci 2015;16:29207-29218. https://doi.org/10.3390/ijms161226156

55. Xu L, Kitade H, Ni Y, Ota T. Roles of chemokines and chemokine receptors in obesity-associated insulin resistance and nonalcoholic fatty liver disease. Biomolecules 2015;5:1563-1579. https://doi.org/10.3390/biom5031563

56. Kuroda S, Tashiro H, Kimura Y, Hirata K, Tsutada M, Mikuriya Y, Kobayashi T, ET AL. Rho-kinase inhibitor targeting the liver prevents ischemia/reperfusion injury in the steatotic liver without major systemic adversity in rats. Liver Transpl 2015;21:123-131. https://doi.org/10.1002/lt.24020

57. Anegawa G, Kawanaka H, Yoshida D, Konishi K, Yamaguchi S, Kinjo N, Taketomi A, ET AL. Defective endothelial nitric oxide synthase signaling is mediated by rho-kinase activation in rats with secondary biliary cirrhosis. Hepatology 2008;47:966-977. https://doi.org/10.1002/hep.22089

58. Takeda K, Jin MB, Fujita M, Fukai M, Sakurai T, Nakayama M, Taniguchi M, ET AL. A novel inhibitor of Rho-associated protein kinase, Y-27632, ameliorates hepatic ischemia and reperfusion injury in rats. Surgery 2003;133:197-206. https://doi.org/10.1067/msy.2003.59

59. Kanda T, Wakino S, Homma K, Yoshioka K, Tatematsu S, Hasegawa K, Takamatsu I, ET AL. Rho-kinase as a molecular target for insulin resistance and hypertension. FASEB J 2006;20:169-171. https://doi.org/10.1096/fj.05-4197fje

60. Jahani V, Kavousi A, Mehri S, Karimi G. Rho kinase, a potential target in the treatment of metabolic syndrome. Biomed Pharmacother 2018;106:1024-1030. https://doi.org/10.1016/j.biopha.2018.07.060

61. Noda K, Nakajima S, Godo S, Saito H, Ikeda S, Shimizu T, Enkhjargal B, ET AL. Rho-kinase inhibition ameliorates metabolic disorders through activation of AMPK pathway in mice. PLoS One 2014;9:e110446. https://doi.org/10.1371/journal.pone.0110446

62. Zhang Q-Q, Lu L-G. Nonalcoholic fatty liver disease: dyslipidemia, risk for cardiovascular complications, and treatment strategy. J Clin Transl Hepatol 2015;3:78. https://doi.org/10.14218/JCTH.2014.00037

63. Noguchi M, Hosoda K, Fujikura J, Fujimoto M, Iwakura H, Tomita T, Ishii, T, ET AL. Genetic and pharmacological inhibition of Rho-associated kinase II enhances adipogenesis. J Biol Chem 2007;282:29574-29583. https://doi.org/10.1074/jbc.M705972200

64. Alosco ML, Gunstad J. The negative effects of obesity and poor glycemic control on cognitive function: a proposed model for possible mechanisms. Curr Diab Rep 2014;14:1-7. https://doi.org/10.1007/s11892-014-0495-z

65. Mamdouh M, Shaban S, Ibrahim Abushouk A, Zaki MMM, Ahmed OM, Abdel-Daim MM. Adipokines: potential therapeutic targets for vascular dysfunction in type II diabetes mellitus and obesity. J Diabetes Res 2017;2017:8095926. https://doi.org/10.1155/2017/8095926

66. Ma Z, Zhang J, Du R, Ji E, Chu L. Rho kinase inhibition by fasudil has anti-inflammatory effects in hypercholesterolemic rats. Biol Pharm Bull 2011;34:1684-1689. https://doi.org/10.1248/bpb.34.1684

67. Uchida T, Honjo M, Yamagishi R, Aihara M. The anti-inflammatory effect of ripasudil (K-115), a Rho kinase (ROCK) inhibitor, on endotoxin-induced uveitis in rats. Invest Ophthalmol Visual Sci 2017;58:5584-5593. https://doi.org/10.1167/iovs.17-22679

68. Hofni A, Shehata Messiha BA, Mangoura SA. Fasudil ameliorates endothelial dysfunction in streptozotocin-induced diabetic rats: a possible role of Rho kinase. Naunyn Schmiedebergs Arch Pharmacol 2017;390:801-811. https://doi.org/10.1007/s00210-017-1379-y

69. Takemoto M, Liao JK. Pleiotropic effects of 3-hydroxy-3-methylglutaryl coenzyme a reductase inhibitors. Arterioscler Thromb Vasc Biol 2001;21:1712-1719. https://doi.org/10.1161/hq1101.098486

70. Besse-Patin A, Léveillé M, Oropeza D, Nguyen BN, Prat A, Estall JL. Estrogen signals through peroxisome proliferator-activated Receptor− γ coactivator 1α to reduce oxidative damage associated with diet-induced fatty liver disease. Gastroenterology 2017;152:243-256. https://doi.org/10.1053/j.gastro.2016.09.017

71. García-Ruiz I, Solís-Muñoz P, Fernández-Moreira D, Grau M, Colina F, Muñoz-Yagüe T, Solís-Herruzo JA. High-fat diet decreases activity of the oxidative phosphorylation complexes and causes nonalcoholic steatohepatitis in mice. Dis Model Mech 2014;7:1287-1296. https://doi.org/10.1242/dmm.016766

72. Zhang R, Chu K, Zhao N, Wu J, Ma L, Zhu C, Chen X, ET AL. Corilagin alleviates nonalcoholic fatty liver disease in high-fat diet-induced C57BL/6 mice by ameliorating oxidative stress and restoring autophagic flux. Front Pharmacol 2020;10:1693. https://doi.org/10.3389/fphar.2019.01693

73. Urbanova M, Mraz M, Ďurovcová V, Trachta P, Kloučková J, Kavalkova P, Haluzíková D, ET AL. The effect of very-low-calorie diet on mitochondrial dysfunction in subcutaneous adipose tissue and peripheral monocytes of obese subjects with type 2 diabetes mellitus. Physiol Res 2017;66:811-822. https://doi.org/10.33549/physiolres.933469

74. Guan P, Liang Y, Wang N. Fasudil alleviates pressure overload-induced heart failure by activating Nrf2-mediated antioxidant responses. J Cell Biochem 2018;119:6452-6460. https://doi.org/10.1002/jcb.26662

75. Guo R, Liu B, Zhou S, Zhang B, Xu Y. The protective effect of fasudil on the structure and function of cardiac mitochondria from rats with type 2 diabetes induced by streptozotocin with a high-fat diet is mediated by the attenuation of oxidative stress. Biomed Res Int 2013;2013:430791. https://doi.org/10.1155/2013/430791

76. Mota M, Banini BA, Cazanave SC, Sanyal AJ. Molecular mechanisms of lipotoxicity and glucotoxicity in nonalcoholic fatty liver disease. Metabolism 2016;65:1049-1061. https://doi.org/10.1016/j.metabol.2016.02.014

77. Kanda T, Matsuoka S, Yamazaki M, Shibata T, Nirei K, Takahashi H, Kaneko T, ET AL. Apoptosis and non-alcoholic fatty liver diseases. World J Gastroenterol 2018;24:2661. https://doi.org/10.3748/wjg.v24.i25.2661

78. Thorlacius K, Slotta JE, Laschke MW, Wang Y, Menger MD, Jeppsson B, Thorlacius A. Protective effect of fasudil, a Rho-kinase inhibitor, on chemokine expression, leukocyte recruitment, and hepatocellular apoptosis in septic liver injury. J Leukoc Biol 2006;79:923-931. https://doi.org/10.1189/jlb.0705406

79. Ikeda H, Kume Y, Tejima K, Tomiya T, Nishikawa T, Watanabe N, Ohtomo N, ET AL. Rho-kinase inhibitor prevents hepatocyte damage in acute liver injury induced by carbon tetrachloride in rats. Am J Physiol Gastrointest Liver Physiol 2007;293:G911-G917. https://doi.org/10.1152/ajpgi.00210.2007